

Are your MRI contrast agents cost-effective?

Learn more about generic Gadolinium-Based Contrast Agents.



FRESENIUS  
KABI

caring for life

**AJNR**

**Apparent Diffusion Coefficient of Glial Neoplasms: Correlation with Fluorodeoxyglucose–Positron-Emission Tomography and Gadolinium-Enhanced MR Imaging**

This information is current as of April 17, 2024.

A.I. Holodny, S. Makeyev, B.J. Beattie, S. Riad and R.G. Blasberg

*AJNR Am J Neuroradiol* 2010, 31 (6) 1042-1048

doi: <https://doi.org/10.3174/ajnr.A1989>

<http://www.ajnr.org/content/31/6/1042>

ORIGINAL  
RESEARCH

A.I. Holodny  
S. Makeyev  
B.J. Beattie  
S. Riad  
R.G. Blasberg



# Apparent Diffusion Coefficient of Glial Neoplasms: Correlation with Fluorodeoxyglucose–Positron-Emission Tomography and Gadolinium-Enhanced MR Imaging

**BACKGROUND AND PURPOSE:** Gd-enhancement provides essential information in the assessment of brain tumors. However, enhancement does not always correlate with histology or disease activity, especially in the setting of current therapies. Our aim was to compare FDG-PET scans to ADC maps and Gd-enhanced MR images in patients with glial neoplasms to assess whether DWI might offer information not available on routine MR imaging sequences and whether such findings have prognostic significance.

**MATERIALS AND METHODS:** Institutional review board approval was obtained for this retrospective review, which was conducted in full compliance with HIPAA regulations. Twenty-one patients (11 men and 10 women) with glial tumors underwent FDG-PET and MR imaging, including ADC and Gd-enhancement. Subjectively, regions of interest were drawn around the following areas: 1) increased FDG uptake, 2) decreased signal intensity on ADC maps, and 3) Gd-enhancement. Objectively, FDG-PET and MR images were co-registered, and pixel-by-pixel comparison of ADC to PET values was made for all regions of interest. Correlation coefficients (*r* values) were calculated for each region of interest. Percentage overlap between regions of interest was calculated for each case.

**RESULTS:** Subjective evaluation showed 60% of patients with excellent or good correlation between ADC maps and FDG-PET. Pixel-by-pixel comparison demonstrated *r* values that ranged from  $-0.72$  to  $-0.21$ . There was significantly greater overlap between decreased ADC and increased FDG-PET uptake ( $67.1 \pm 15.5\%$ ) versus overlap between Gd-enhancement and increased FDG-PET uptake ( $54.4 \pm 27.5\%$ ) ( $P < .05$ ). ADC overlap was greater with increased FDG-PET than with Gd-enhancement in 8/9 cases. Survival data revealed that the presence of restricted diffusion on ADC correlated with patient survival ( $P < .0001$ ).

**CONCLUSIONS:** ADC maps in patients with brain tumors provide unique information that is analogous to FDG-PET. There is a greater overlap between ADC and FDG-PET compared with Gd-enhancement. ADC maps can serve to approximate tumor grade and predict survival.

**ABBREVIATIONS:** A = area of restricted diffusion on an ADC map; AA = anaplastic astrocytoma; ADC = apparent diffusion coefficient; AODG = anaplastic oligodendroglioma; d = days; F = area of increased FDG-PET uptake; DWI = diffusion-weighted MR imaging; FDG-PET = fluorodeoxyglucose–positron-emission tomography; FLAIR = fluid-attenuated inversion recovery; G = area of gadolinium enhancement on MR imaging; GBM = glioblastoma multiforme; Gd = gadolinium; Gd-DTPA = gadolinium-diethylene-triamine pentaacetic acid; IPAA = Health Insurance Portability and Accountability Act; LGA = low-grade astrocytoma; LGODG = low-grade oligodendroglioma; m = months; PET = positron-emission tomography; *r* value = correlation coefficient;  $\cap$  = intersection

**G**liomas are the most common primary neoplasms of the central nervous system in adults.<sup>1</sup> The prognosis and treatment strategies vary according to tumor grade.<sup>2</sup> When one is following low-grade tumors, one of the most important events is malignant degeneration, which is triggered by incompletely understood molecular mechanisms.<sup>3–5</sup> Malignant degeneration leads to a worsening of the prognosis and often to a change in the clinical management.<sup>2</sup>

Routine Gd-enhanced MR imaging plays a crucial role in

the assessment of gliomas.<sup>6</sup> However, Gd-enhancement has limitations in that it identifies the presence of an abnormal blood-brain barrier,<sup>7</sup> rather than physiology, histology, genetic aberrations, or molecular events. With the advent of molecular and genetic treatment strategies aimed at gliomas,<sup>3,4</sup> more sophisticated radiologic methods are necessary to follow these tumors, including assessment of therapy and the detection of tumor progression.

FDG-PET possesses the unique ability among imaging studies to depict and quantify glucose metabolism. In tumors, glucose utilization is increased, due to the Warburg effect.<sup>8</sup> The ability of FDG-PET to define this physiologic state, as opposed to the structural imaging of routine MR images, has been shown to be of use in the study of gliomas, including the degree of malignancy,<sup>9</sup> prognosis,<sup>9,10</sup> the evaluation of early recurrence and malignant transforma-

Received November 10, 2008; accepted after revision October 31, 2009.

From the Departments of Radiology (A.I.H., S.M. S.R.) and Neurology (B.J.B., R.G.B.), Memorial Sloan-Kettering Cancer Center, New York, New York.

Please address correspondence to Andrei I. Holodny, MD, Department of Radiology, Memorial Sloan-Kettering Cancer Center, 1275 York Ave, New York, NY 10021; e-mail: holodnya@mskcc.org

DOI 10.3174/ajnr.A1989

tion,<sup>11-13</sup> and differentiating tumor recurrence from radiation necrosis.<sup>14-16</sup>

ADC maps obtained from DWI can also provide physiologic information by detecting regional variation in the diffusion of free water within brain tissue. Prior studies have reported mixed results as to the utility of ADC maps in establishing the grade of glioma, with some authors finding a correlation between glioma grade and ADC<sup>17-20</sup> and others not finding ADC maps useful.<sup>21-23</sup> Moreover, Murakami et al<sup>24</sup> found a correlation between pretreatment minimum ADC values and survival in patients with malignant supratentorial astrocytomas. One possible reason for the discrepancy in the efficacy of ADC in establishing the grade of gliomas may be in the placement of regions of interest, with those authors who placed generous regions of interest encompassing the entire tumor not finding a correlation<sup>21</sup> and those identifying specific areas within the tumor (in most articles defined as “minimum ADC”) able to establish significance.<sup>19,25</sup>

ADC maps have recently been correlated with FDG-PET in non-neurologic malignancies<sup>26,27</sup> as well as in brain metastases.<sup>28</sup> We, therefore, hypothesized that we would be able to establish a correlation between ADC and FDG-PET by using a voxel-by-voxel analysis of glial tumors, with those areas of the tumor exhibiting the lowest ADC values correlating with areas of highest uptake of FDG-PET. We further hypothesized that a comparison of the overlap of FDG-PET and ADC to the overlap of Gd-enhancement to ADC would establish that ADC provided information analogous to FDG-PET, which was not available on routine anatomic MR imaging sequences. Using survival data, we also tested the hypothesis that positive findings on ADC and FDG-PET would correlate better with patient outcomes than Gd-enhanced MR imaging.

## Materials and Methods

Institutional review board approval was obtained for this retrospective review, which was conducted in full compliance with HIPAA regulations.

### Patient Population

A retrospective review was conducted on all patients at our institution with pathologically confirmed glial tumors of the brain who underwent MR imaging and FDG-PET within 4 weeks of each other during an 18-month period. Twenty-two consecutive patients were identified. One patient was excluded because the DWI sequence was not performed, leaving a total of 21 patients. The patients ranged in age from 20 to 79 years (average,  $46 \pm 12$  years). There were 11 men and 10 women. The diagnosis was pathologically confirmed in all patients. There were 5 glioblastoma multiforme, 5 anaplastic astrocytomas, 2 anaplastic oligodendrogliomas, 6 low-grade astrocytomas, and 3 low-grade oligodendrogliomas (Table 1).

### Scans

All patients underwent MR imaging on a 1.5T scanner (Signa LX; GE Healthcare, Milwaukee, Wisconsin) by using a quadrature head coil. DWI (TR = 10,000, TE = 100) was performed in 3 orthogonal planes with a *b*-value of 1000 s/mm<sup>2</sup>, 5-mm-thick sections with a 2.5-mm skip, a 128 × 128 matrix, and an FOV of 24 cm. ADC maps were calculated by using FuncTool software (GE Healthcare).<sup>29</sup> ADC maps were evaluated instead of the DWIs for this study to eliminate the “shine-through” effect seen on the latter.<sup>30</sup>

**Table 1: Patient population**

Patient	Tumor	Age (yr)	Sex	Survival from Date of	
				Diagnosis	Imaging
1	GBM	31	M	10 m 26 d	11 m 5 d
2	GBM	36	F	11 m 13 d	10 m 19 d
3	GBM	49	M	6 m 12 d	7 m 2 d
4	GBM	56	F	12 m 8 d	6 m 20 d
5	GBM	56	M	29 m 19 d	15 m 19 d
6	AA	20	F	35 m 6 d	25 d
7	AA	50	F	17 m 3 d	5 m 22 d
8	AA	49	M	10 m 30 d	7 m 25 d
9	AA	45	M	7 m 15 d	9 m 7 d
10	AA	51	F	21 m	6 m 18 d
11	AODG	43	M	81 m 14 d	65 m 11 d
12	AODG	41	M	63 m 6 d	41 m 10 d
13	LGA	51	F	>76 m	>75 m
14	LGA	35	F	53 m 17 d	39 m 16 d
15	LGA	49	M	>157 m	>86 m
16	LGA	54	M	>127 m	>78 m
17	LGA	79	F	>105 m	>74 m
18	LGODG	42	F	50 m 14 d	49 m 1 d
19	LGODG	34	F	125 m 5 d	25 m 11 d
20	LGODG	47	M	21 m 15 d	15 m 4 d
21	LGA	45	M	48 m 14 d	40 m 9 d

Before injection of Gd-DTPA, we performed the following anatomic sequences: sagittal T1-weighted (TR = 600, TE = 15), axial T2-weighted (TR = 4000, TE = 102), FLAIR (TR = 10,000, TE = 160), and T1-weighted imaging (TR = 500, TE = 15). Following the injection of intravenous Gd-DTPA (0.1 mmol/kg), axial T1-weighted (TR = 500, TE = 15) and coronal T1-weighted (TR = 500, TE = 15) images were obtained. All of these were obtained with 5-mm-thick sections with a 2.5-mm skip, a 256 × 256 matrix, and an FOV of 24 cm.

None of the patients had a change in chemotherapy or received radiation therapy within the past 3 months. All of the FDG-PET scans were obtained to answer the clinical questions of whether there was progression of disease. None of the FDG-PET scans were obtained to evaluate therapy. The PET scans were obtained 30 minutes following the intravenous injection of approximately 10 mCi of 2-<sup>18</sup>F-fluoro-2-deoxy-D-glucose.

The FDG-PET and MR imaging were performed within 2 weeks of each other (except 1 at 4 weeks and 1 at 3 weeks), average  $1.3 \pm 1.1$  weeks. There was no change in the clinical status of the patient between the scanning.

All image registrations were obtained through the application of a 6-parameter rigid-body transformation matrix followed by trilinear interpolation. Each transformation matrix, in turn, was determined by using a nonlinear gradient search that sought to maximize a normalized mutual information cost function applied to the voxel intensities of each registered 3D image pair.<sup>31</sup> The software implementing this procedure, minctracc, is available from the McConnell Brain Imaging Centre of the Montreal Neurologic Institute.<sup>32</sup> Transforms were calculated to map the FDG-PET and each of the axial MR imaging sequences, DWI, T2, FLAIR, and postcontrast T1 to the precontrast T1-weighted images, thus, by proxy, registering all of these scans to one another.

### Subjective Evaluation

All MR images and PET scans underwent a subjective evaluation by a fellowship-trained neuroradiologist and nuclear medicine physician respectively. The MR images were evaluated for Gd-

**Table 2: Summary of imaging results and overlap<sup>a</sup>**

Patient	PET	ADC	Gd	1	2	3	4	5	6	R Value
				A ∩ F / A	A ∩ F / F	A ∩ F / AF	G ∩ F / G	G ∩ F / F	G ∩ F / GF	
1	+	+	+	58.1	81	51.2	15.5	69.5	14.5	0.369
2	+	+	+	58.8	34.5	48.7	41.8	80	37.9	-0.629
3	+	+	+	63.6	56.2	42.5	30.7	66.7	26.6	-0.66
4	+	+	+	85	71.8	64	82.3	60.3	53.4	-0.686
5	+	+	-	55.8	71.4	45.7	-	-	-	-0.125
6	+	+	+	72.6	76.3	59.4	46.7	83.8	42.9	-0.722
7	+	+	+	88	73	66.8	74.1	78.7	61.8	-0.451
8	+	+	+	84	81.5	70.8	87	75.1	67.5	-0.207
9	+	+	+	46.8	40.6	27.7	44.1	72.7	37.8	-0.28
10	+	+	+	54.6	74.8	46.1	31.6	48.7	23.8	-0.38
11	-	-	-	-	-	-	-	-	-	-0.222
12	+	-	+	-	-	-	38	44.9	25.9	-0.044
13	-	-	-	-	-	-	-	-	-	0.59
14	-	-	-	-	-	-	-	-	-	0.015
15	-	-	-	-	-	-	-	-	-	-0.569
16	-	-	-	-	-	-	-	-	-	-0.0569
17	-	-	-	-	-	-	-	-	-	-0.611
18	-	-	-	-	-	-	-	-	-	0.201
19	-	-	-	-	-	-	-	-	-	-0.319
20	-	-	-	-	-	-	-	-	-	-0.006
21	-	-	-	-	-	-	-	-	-	-0.469

<sup>a</sup> + indicates subjective evaluation of positive findings on imaging; -, no findings on imaging. See "Materials and Methods" for further explanation of Table values and their derivation.

enhancement and decreased ADC signal intensity (restricted diffusion). ADC maps of tumors generally have increased signal intensity in the area of the tumor. Consequently, restricted diffusion in the area of the tumor was defined as decreased signal intensity with respect to the generally increased ADC signal intensity seen in the tumor, not with respect to normal contralateral white matter. For the purpose of this exercise, the volume of the tumor was defined as the volume of abnormally increased signal intensity on the FLAIR sequence. The FDG-PET scans were evaluated for increased radiopharmaceutical uptake.

A subjective evaluation was made of the degree of overlap between above 3 variables, increased FDG-PET uptake, restricted diffusion on ADC maps, and Gd-enhancement, and was graded as excellent, good, mild, or none.

### Objective Evaluation

A pixel-by-pixel comparison between the FDG-PET scan and the ADC maps was made of the entire volume of the tumor and peritumoral edema. The volume of tumor and surrounding edema was defined as the volume of abnormally increased signal intensity on the FLAIR sequence. A graph of this relationship was plotted and a correlation coefficient was obtained for the 2 values for each patient.

Regions of interest were drawn manually around the following areas for each patient: 1) increased FDG-PET uptake, 2) decreased signal intensity on the ADC maps (this area was defined in exactly the same manner as in the "Subjective Evaluation" section), and 3) Gd-enhancement on the T1-weighted images. Each of these regions of interest was drawn blindly, in that the person drawing them was not aware of the position of regions of interest for the other parameters.

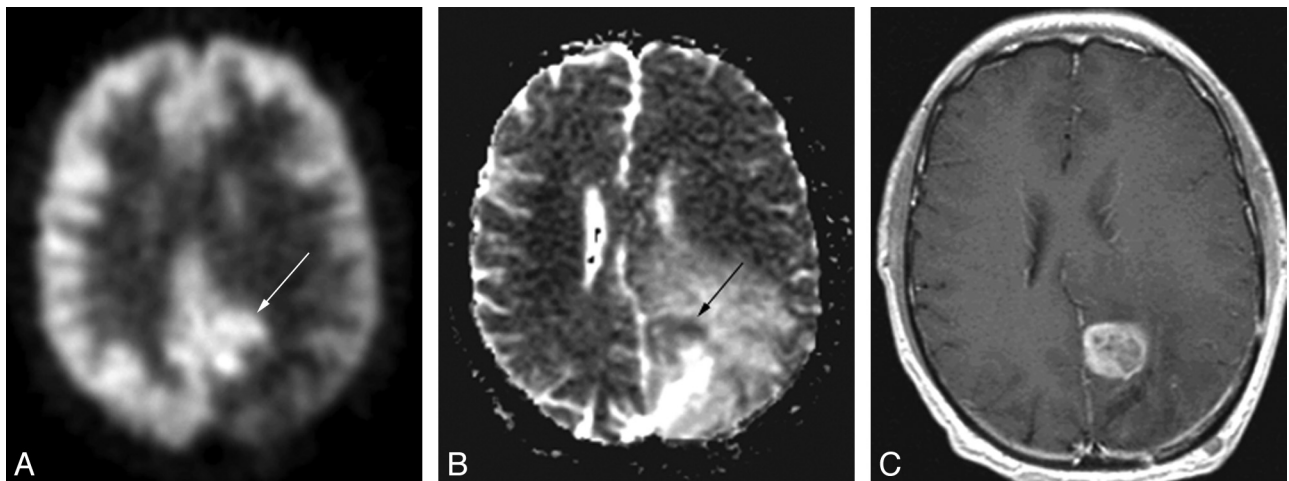


**Fig 1.** A 49-year-old man with an anaplastic astrocytoma. The PET scan (A) demonstrates a C-shaped area of increased radiopharmaceutical uptake (arrow), which exquisitely matches the area of restricted diffusion on the ADC map (arrow, B). C, The correspondence between the FDG-PET scan and the ADC map is better than that in the gadolinium-enhanced MR image (C).

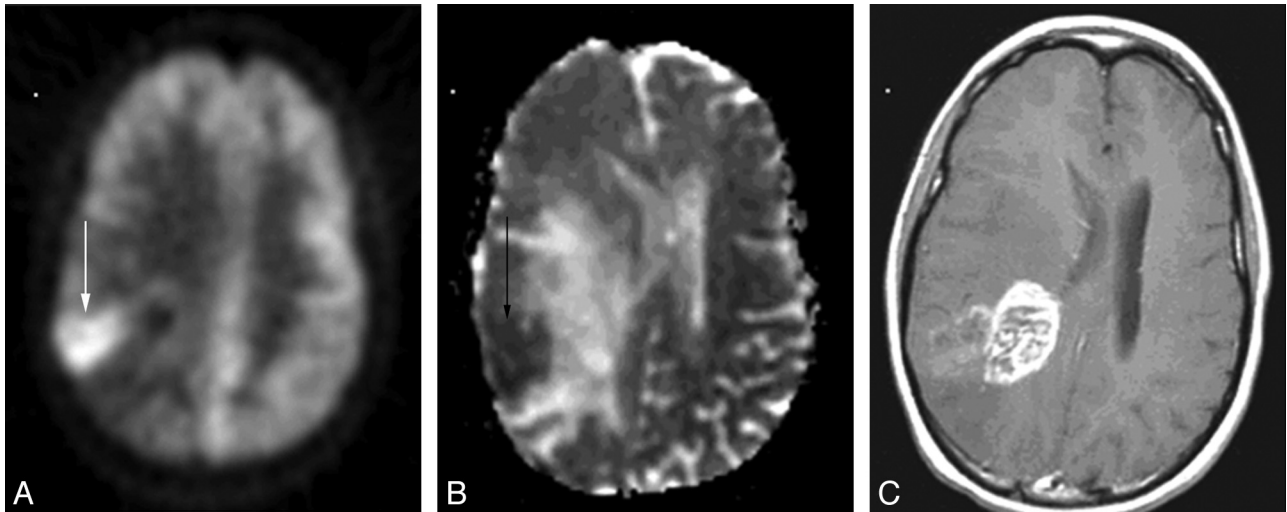


**Fig 2.** A 20-year-old woman with an anaplastic astrocytoma. The area of FDG-PET (arrow, A) uptake closely matches the area of restricted diffusion on the ADC map (arrow, B). This area only shows subtle enhancement (C). The area of bright enhancement does not correlate with either increased FDG-PET uptake or restricted diffusion.

The percentage overlap was calculated for each patient for the various regions of interest in the following manner:

$$1) \quad A \cap F / A = (ADC \cap FDG) \div ADC \times 100\%,$$

where  $ADC \cap FDG$  means the number of pixels that are common to both ADC and FDG regions of interest. This value is divided by the total number of pixels in the region of interest for ADC. If the regions of interest for ADC and FDG completely overlap, the value for 1 will be 100. If there is not overlap, the value will be zero. The other percentages of overlap were calculated in a similar manner, as follows:

$$2) \quad A \cap F / F = (ADC \cap FDG) \div FDG \times 100\%$$

$$3) \quad A \cap F / AF = (ADC \cap FDG) \div (ADC + FDG) \times 100\%$$

$$4) \quad G \cap F / G = (Gd \cap FDG) \div Gd \times 100\%$$

$$5) \quad G \cap F / F = (Gd \cap FDG) \div FDG \times 100\%$$

$$6) \quad G \cap F / GF = (Gd \cap FDG) \div (FGD + Gd) \times 100\%.$$

The above parameters were compared by using a Student *t* test.

### Patient Survival

The time each patient survived following the MR imaging and PET was determined. The survival data for each of the subjective imaging modalities described above was presented by using Kaplan-Meier curves. The survival curves were compared by using the Student *t* test. Significance was set at  $P < .05$  (Fig 3).

## Results

### Subjective Evaluation

Eleven patients presented with areas of increased FDG-PET uptake (patients 1–10 and 12). Of these, scans of 10 patients had decreased ADC signal intensity (patients 1–10), and those of 10 patients had Gd-enhancement of the tumor (patients 1–9 and 12) (Table 2).

Scans of 6 of the 10 patients had excellent or good correlation between increased FDG-PET uptake and decreased ADC (Fig 1). Four had a mild correlation. The subjective evaluation

also showed a better correlation between FDG-PET and ADC than between FDG-PET and Gd-enhancement. This was most dramatic in 1 case in which there was an excellent overlap between the FDG-PET and the ADC, but Gd-enhancement was confined to a different area (Fig 2).

### Objective Evaluation

For those patients with both increased uptake on FDG-PET and decreased signal intensity on ADC maps, the correlation coefficient (*r* value) between the 2 ranged from  $-0.722$  to  $-0.207$  (average =  $-0.487 \pm 0.191$ ). Four of these patients, all of whom had glioblastomas, had *r* values greater than  $-0.62$  (Table 2).

The results for the overlap of the regions of interest drawn for the areas of increased radiopharmaceutical uptake on FDG-PET, areas of restricted diffusion as seen on the ADC maps, and the areas of Gd-enhancement are also presented in Table 2.

The values in column 1 (the intersection of FDG-PET with ADC normalized to ADC) were greater than those in column 4 (the intersection of FDG-PET with Gd-enhancement normalized to Gd-enhancement) in all cases except 1 (89%). Therefore, with this method, the overlap between FDG-PET and ADC was greater than for Gd in 89% of the cases. The average overlap was also greater for FDG-PET and ADC ( $67.1 \pm 15.5\%$ ) than for FDG-PET and Gd ( $54.4 \pm 27.5\%$ ) ( $P < .05$ ).

The same can be said when one compares the values for column 3 (the intersection of FDG-PET with ADC normalized to the sum of FDG-PET and ADC) with those in column 6 (the intersection of Gd-enhancement with FDG-PET normalized to the sum of Gd and FDG-PET). The values in column 3 were greater than those in column 6 in all cases except for 1 (89%). Therefore, with this method, the overlap between FDG-PET and ADC was greater than that for Gd in 89% of the cases. The average overlap was also greater for FDG-PET and ADC ( $53.6 \pm 14.1\%$ ) than for Gd- and FDG-PET ( $36.2 \pm 19.3\%$ ). This did not reach statistical significance ( $P < .09$ ).

However, when one normalizes to FDG-PET, the results

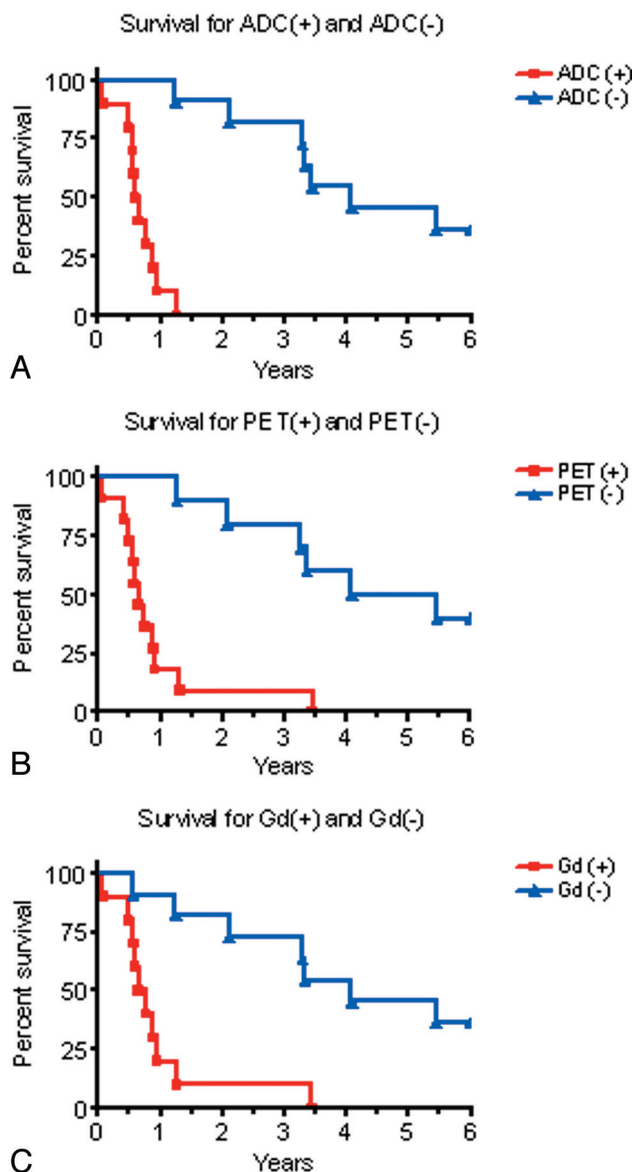


**Fig 3.** *Top*, Survival curves for the 10 patients with restricted diffusion on ADC maps and for the 11 patients without restricted diffusion on ADC maps,  $P < .0001$ . *Middle*, Survival curves for the 11 patients with increased FDG uptake on PET and the 10 patients with no increased FDG uptake on PET,  $P = .0004$ . *Bottom*, Survival curves for the 10 patients with gadolinium enhancement and the 11 patients without gadolinium enhancement.

are different. The values in column 2 (the intersection of FDG-PET with ADC normalized to FDG-PET) were greater than those in column E (the intersection of FDG-PET with Gd-normalized to FDG-PET) in only 4 of the cases (45%). There was no statistically significant difference between the average values:  $66.7 \pm 17.3\%$  versus  $61.9 \pm 11.6\%$  ( $P < .62$ ).

#### Patient Survival

Significant differences were found for the survival curves in patients with versus those without FDG-PET uptake ( $P = .0004$ ), restricted diffusion on ADC maps ( $P < .0001$ ), and Gd-enhancement ( $P = .0004$ ). There was no statistically significant difference between the survival curves for patients with Gd+, PET+, and ADC+, and no statistically significant difference was seen between survival curves for patients with Gd-, PET-, and ADC- (Fig 3).

#### Discussion

The data demonstrate that there is a large overlap between increased FDG-PET uptake and restricted diffusion as measured by ADC maps. In a number of cases, the overlap was striking. For example, in patient 6, the  $r$  value was  $-0.722$ . In other cases, the correlation was much weaker. In addition, the overlap between ADC and FDG-PET was greater than that between FDG-PET and Gd-enhancement. In a number of cases, there was a strong overlap between ADC and FDG-PET, with a weak or absent overlap between FDG-PET and Gd-enhancement (Figs 1 and 2). Our results indicate that ADC maps may provide information similar to that in FDG-PET that is not present on Gd-enhanced scans.

#### Possible Explanations

Given the fact that FDG-PET and ADC measure different physiologic parameters, the strong overlap between these 2 parameters may be viewed as somewhat surprising. We will explore 2 possible explanations for these results.

**Increased Metabolism and Increased Cellularity.** Increased FDG-PET uptake measures increased glycolysis, which is due to increased metabolic activity in high-grade tumors, a phenomenon known as the Warburg effect.<sup>8</sup> Areas of high cellularity contain more cell membranes than normal brain, leading to greater impedance to the diffusion of water molecules. Tumors that tend to be highly cellular, such as lymphomas, tend to have decreased signal intensity on ADC maps.<sup>33</sup>

Our findings demonstrate an overlap between increased FDG-PET uptake and increased signal intensity on ADC. It is possible that areas of increased metabolic activity (increased FDG-PET uptake) correspond well to areas of high tumor cellularity (restricted diffusion on ADC).

**Ischemia.** Another possible explanation for the presented data is ischemia. Increased FDG-PET uptake can also reflect increased glycolysis due to focal ischemia.<sup>12,34,35</sup> In high-grade glial tumors, the areas of ischemia would be located where the increasing metabolic demands of rapidly growing cells are outstripping the vascular supply, causing the cells to switch to glycolysis.

Restricted diffusion of water in areas of high-grade tumor is thought to be due to increased cell attenuation; however, this restricted diffusion could also reflect areas of focal ischemia and irreversible cell death. As malignant degeneration occurs, the rapidly dividing cells begin to outgrow their blood supply, leading to ischemia and eventual cell death. It is well known from diffusion imaging of stroke that cells in the early stages of irreversible ischemia demonstrate restricted diffusion.<sup>36-40</sup> Ischemic cells in a brain tumor also likely demonstrate decreased signal intensity on the ADC maps.

Presumably, the cells in a malignant glioma that are outgrowing their blood supply (increased FDG-PET signal intensity) would be directly adjacent to the cells that have crossed the irreversible ischemia barrier and demonstrate restricted diffusion (decreased signal intensity on the ADC maps). Therefore, the high correlation of increased FDG-PET uptake and decreased signal intensity on an ADC map may be due to the consequences of ischemia.

### **Possible Clinical Application**

From the current results, it is unclear which of the above mechanisms or combinations thereof are correct. However, the results suggest that ADC maps may provide information about the physiologic state of a tumor that is complementary to that obtained with FDG-PET and is not reflected on the Gd-enhanced T1 images. Of all of routine MR imaging sequences, it appears that the indirect information about cell attenuation and/or ischemia may be uniquely provided by the diffusion sequence. In any of the scenarios described above, the information provided by the ADC map appears to point to cellular and molecular mechanisms that are the consequences of malignant degeneration.

### **Patient Survival**

Higano et al<sup>19</sup> demonstrated that in patients with GBM or AA, minimum ADC value within the tumor is related to patient prognosis: Lower minimum ADC values are associated with higher levels of Ki-67–positive cells (a marker of malignancy) and shorter survival times. Our data demonstrating shorter survival times in patients with areas of restricted diffusion (ie, low ADC values) support the idea that ADC maps can be used to determine clinical malignancy and patient prognosis.

The survival data of the admittedly small number of patients suggests that ADC and FDG-PET may be more predictive of the clinical course than Gd-enhanced MR imaging. Patient 10, having restricted diffusion on ADC maps and increased FDG-PET uptake, had no Gd-enhancement and survived for only 6 months after imaging.

Findings on ADC and FDG-PET were consistent with one another across all patients except for Patient 12. Patient 12 was the only one in the cohort who presented with a large area of prominent increased FDG-PET uptake, strong Gd-enhancement, but no restricted diffusion on the ADC maps. He was rather atypical in that though he had prominent uptake on FDG-PET, he survived for 3 years. Usually such patients die much more quickly.<sup>9,12</sup> It may be argued in this case that the ADC map was a more accurate indicator of the true biology of the tumor and a lack of aggressive malignant transformation than the FDG-PET scan or the Gd-enhanced MR imaging.

### **Other Causes for Restricted Diffusion**

Restricted diffusion has also been reported in glial tumors in both animals<sup>40,41</sup> and humans following successful therapy and reduction in the size of the tumor.<sup>42–47</sup> These reports stated that the restricted diffusion reflected the actual death of tumor cells. However, the current study was performed in a completely different clinical setting. Here, PET and MR imaging were performed to determine if there was tumor progression, not to monitor the effectiveness of a new therapy. Also, it would be unlikely for an area of the tumor that was being treated successfully to develop increased FDG-PET uptake.

From the point of view of interpreting the images from a clinical MR image in a patient with a glioma and an area of restricted diffusion on the ADC map, the radiologist would have to consider both possibilities: The findings may be due to successful treatment effect or malignant transformation. In such cases, the clinical history would serve as a valuable ad-

duct. If the patient had recently undergone a new aggressive therapy, one may lean toward the restricted diffusion representing treatment effect. On the other hand, if the patient who was not being treated or was continuing previous treatment developed an area of restricted diffusion, one should consider malignant transformation.

### **Limitations**

The current study is limited in that the areas of tumor that showed different FDG-PET, ADC, and Gd-enhancement characteristics were not analyzed histologically, immunohistochemically, or by molecular or genetic probes. Therefore, one cannot draw conclusions regarding the relationship of restricted diffusion on ADC to the above parameters or to other measurements of malignancy. Also, ADC values were correlated to FDG-PET at 1 point in time. We did not follow ADC values with time to see how they changed as the tumor progressed. Consequently, we did not evaluate which of the radiologic parameters correlated best with malignant degeneration of the tumor.

The group studied was heterogeneous in that we studied grade II through IV gliomas. Most of the low-grade tumors exhibited none of the radiologic markers of malignancy (restricted diffusion, Gd-enhancement, or FDG uptake). The number of malignant tumors was small, so it was difficult to establish whether some of our findings were spurious or reflective of a general trend. For example, there was a single case in which ADC and FDG-PET were apparently better predictors for survival than Gd-enhancement (patient 10) and another case where ADC was also apparently a better predictor of survival than either FDG-PET or Gd-enhancement (patient 12).

In addition to the heterogeneity of the tumor grade, the treatments which the patients received were also heterogeneous as these treatments were dictated by their clinical course. The FDG-PET and MR imaging scans, obtained within 2 weeks of each other (except one at 4 weeks and one at 3 weeks), average  $1.3 \pm 1.1$  weeks. Notwithstanding a lack of change in the clinical status of the patient between the scans, there is a possibility that the patient's disease progressed during the interval between the MR imaging and PET scans.

It should be noted that none of the imaging parameters can serve as absolute predictors of survival. For example, patient 20 did not demonstrate positive findings on any of the 3 imaging parameters but only survived for 15 months and 4 days, which is shorter than patient 5 with a GBM and positive PET and ADC findings (who survived for 15 months and 19 days) and patient 12 with an AODC and positive PET and Gd-enhancement (who survived for 41 months and 10 days).

### **Conclusions**

The pixel-by-pixel correlation between ADC maps and FDG-PET uptake was varied and ranged between excellent ( $-0.722$ ) and mild ( $-0.207$ ). ADC maps overlapped better with FDG-PET than with Gd-enhancement. Therefore, ADC maps in patients with gliomas appear to provide unique information that is analogous to FDG-PET, which is occasionally not appreciated on Gd-enhanced MR imaging sequences. ADC maps

can serve as a noninvasive method of approximating tumor grade and predicting patient survival.

## References

1. Burger PC, Vogel FS. **The brain: tumors.** In: Burger PC, Vogel FS, eds. *Surgical Pathology of the Central Nervous System and Its Coverings.* New York: Wiley; 1982:223–66
2. DeAngelis L. **Brain tumors.** *N Engl J Med* 2003;344:114–23
3. Hesselager G, Holland EC. **Using mice to decipher the molecular genetics of brain tumors.** *Neurosurgery* 2003;53:685–94
4. Dai C, Holland EC. **Astrocyte differentiation states and glioma formation.** *Cancer J* 2003;9:72–81
5. Fomchenko EI, Holland EC. **Mouse models of brain tumors and their applications in preclinical trials.** *Clin Cancer Res* 2006;12:5288–97
6. Felix R, Schorner W, Laniado M, et al. **Brain tumors: MR imaging with gadolinium-DTPA.** *Radiology* 1985;156:681–88
7. Brasch RC, Weinmann HJ, Wesbey GE. **Contrast-enhanced NMR imaging: animal studies using gadolinium-DTPA complex.** *AJR Am J Roentgenol* 1984;142:625–30
8. Warburg O. **On the origin of cancer cells.** *Science* 1956;123:309–14
9. Coleman RE, Hoffman JM, Hanson MW, et al. **Clinical application of PET for the evaluation of brain tumors.** *J Nucl Med* 1991;32:616–22
10. Barker FG, Chang SM, Valk PE, et al. **18-Fluorodeoxyglucose uptake and survival of patients with suspected recurrent malignant glioma.** *Cancer* 1997;79:115–26
11. Glantz MJ, Hoffman JM, Coleman RE, et al. **Identification of early recurrence of primary central nervous system tumors by [18F]fluorodeoxyglucose positron emission tomography.** *Ann Neurol* 1991;29:347–55
12. Ishikawa M, Kikuchi H, Miyatake S, et al. **Glucose consumption in recurrent gliomas.** *Neurosurgery* 1993;33:28–33
13. Kahn D, Follett KA, Bushnell DL, et al. **Diagnosis of recurrent brain tumor: value of 201Tl SPECT vs 18F-fluorodeoxyglucose PET.** *AJR Am J Roentgenol* 1994;163:1459–65
14. Doyle WK, Budinger TF, Valk PE, et al. **Differentiation of cerebral radiation necrosis from tumor recurrence by [18F]FDG and 82Rb positron emission tomography.** *J Comput Assist Tomogr* 1987;11:563–70
15. Buchpiguel CA, Alavi JB, Alavi A, et al. **PET versus SPECT in distinguishing radiation necrosis from tumor recurrence in the brain.** *J Nucl Med* 1995;36:159–64
16. Deshmukh A, Scott JA, Palmer EL, et al. **Impact of fluorodeoxyglucose positron emission tomography on the clinical management of patients with glioma.** *Clin Nucl Med* 1996;21:720–25
17. Kim HS, Kim SY. **A prospective study on the added value of pulsed arterial spin-labeling and apparent diffusion coefficients in the grading of gliomas.** *AJNR Am J Neuroradiol* 2007;28:1693–99
18. Sugahara T, Korogi Y, Kochi M. **Usefulness of diffusion-weighted MRI with echo-planar technique in the evaluation of cellularity in gliomas.** *J Magn Reson Imaging* 1999;9:53–60
19. Higano S, Yun X, Kumabe T, et al. **Malignant astrocytic tumors: clinical importance of apparent diffusion coefficient in prediction of grade and prognosis.** *Radiology* 2006;241:839–46
20. Fan GG, Deng QL, Wu ZH, et al. **Usefulness of diffusion/perfusion-weighted MRI in patients with non-enhancing supratentorial brain gliomas: a variable tool to predict tumour grading?** *Br J Radiol* 2006;79:652–58
21. Castillo M, Smith JK, Lester k, et al. **Apparent diffusion coefficients in the evaluation of high-grade cerebral gliomas.** *AJNR Am J Neuroradiol* 2001;22:60–64
22. Kono K, Inoue Y, Nakayama K, et al. **The role of diffusion-weighted imaging in patients with brain tumors.** *AJNR Am J Neuroradiol* 2001;22:1081–88
23. Lam WW, Poon WS, Metreweli C. **Diffusion MR imaging in glioma: does it have any role in the pre-operation determination of grading of glioma?** *Clin Radiol* 2002;57:219–25
24. Murakami R, Sugahara T, Nakamura H, et al. **Malignant supratentorial astrocytoma treated with postoperative radiation therapy: prognostic value of pre-treatment quantitative diffusion-weighted MR imaging.** *Radiology* 2007;243:493–99
25. Murakami R, Hirai T, Kitajima M, et al. **Magnetic resonance imaging of pilocytic astrocytomas: usefulness of the minimum apparent diffusion coefficient (ADC) value for differentiation from high-grade gliomas.** *Acta Radiol* 2008;49:462–67
26. Mori T, Nomori H, Ikeda K, et al. **Diffusion-weighted magnetic resonance imaging for diagnosing malignant pulmonary nodules/masses: comparison with positron emission tomography.** *J Thorac Oncol* 2008;3:358–64
27. Ho KC, Lin G, Wang JJ, et al. **Correlation of apparent diffusion coefficients measured by 3T diffusion-weighted MRI and SUV from FDG PET/CT in primary cervical cancer.** *Eur J Nucl Med Mol Imaging* 2009;36:200–08. Epub 2008 Sep 9
28. Palumbo B, Angotti F, Marano GD. **Relationship between PET-FDG and MRI apparent diffusion coefficients in brain tumors.** *Q J Nucl Med Mol Imaging* 2008;52:1–6
29. Le Bihan D, Breton E, Lallemand D, et al. **Separation of diffusion and perfusion in intravoxel incoherent motion MR imaging.** *Radiology* 1998;168:497–505
30. Burdette JH, Elster AD, Ricci PE. **Acute cerebral infarction: quantification of spin-density and T2 shine-through phenomena on diffusion-weighted MR images.** *Radiology* 1999;212:333–39
31. Collington F, Maes D, Delaere D, et al. **Automated multi-modality image registration based on information theory.** *International Conference on Information Processing in Medical Imaging*, IPMI 95, Ile de Berder, France, June 1995;263–74
32. Minctrac. **The McConnell Brain Imaging Centre of the Montreal Neurological Institute.** <http://www.bic.mni.mcgill.ca/ServicesSoftware/HomePage>. Accessed January 25, 2010.
33. Stadnik TW, Chaskis C, Michotte A, et al. **Diffusion-weighted MR imaging of intracerebral masses: comparison with conventional MR imaging and histologic findings.** *AJNR Am J Neuroradiol* 2001;22:969–76
34. Rajendran JG, Mankoff DA, O'Sullivan F, et al. **Hypoxia and glucose metabolism in malignant tumors: evaluation by [18F]fluoromisonidazole and [18F]fluorodeoxyglucose positron emission tomography imaging.** *Clin Cancer Res* 2004;10:2245–52
35. Larson SM. **Positron emission tomography-based molecular imaging in human cancer: exploring the link between hypoxia and accelerated glucose metabolism.** *Clin Cancer Res* 2004;10:2203–04
36. Mintorovitch J, Moseley ME, Chileuitt L, et al. **Comparison of diffusion- and T2-weighted MRI for the early detection of cerebral ischemia and reperfusion in rats.** *Magn Reson Med* 1991;18:39–50
37. Moseley ME, Wendland MF, Kucharczyk J. **Magnetic resonance imaging of diffusion and perfusion.** *Top Magn Reson Imaging* 1991;3:50–67
38. Warach S, Chien D, Li W, et al. **Fast magnetic resonance diffusion-weighted imaging of acute human stroke.** *Neurology* 1992;42:1717–22. Erratum in *Neurology* 1992;42:2192
39. Warach S, Gaa J, Siewert B, et al. **Acute human stroke studied by whole brain echo planar diffusion-weighted magnetic resonance imaging.** *Ann Neurol* 1995;37:231–41
40. Chenevert TL, McKeever PE, Ross BD. **Monitoring early response of experimental brain tumors to therapy using diffusion magnetic resonance imaging.** *Clin Cancer Res* 1997;3:1457–66
41. Valonen PK, Lehtimäki KK, Vaisanen TH, et al. **Water diffusion in a rat glioma during ganciclovir-thymidine kinase gene therapy-induced programmed cell death in vivo: correlation with cell density.** *J Magn Reson Imaging* 2004;19:389–96
42. Chenevert TL, Stegman LD, Taylor JM, et al. **Diffusion magnetic resonance imaging: an early surrogate marker of therapeutic efficacy in brain tumors.** *J Natl Cancer Inst* 2000;92:2029–36
43. Mardor Y, Roth Y, Lidar Z, et al. **Monitoring response to convection-enhanced taxol delivery in brain tumor patients using diffusion-weighted magnetic resonance imaging.** *Cancer Res* 2001;61:4971–73
44. Hein PA, Eskey CJ, Dunn JF, et al. **Diffusion-weighted imaging in the follow-up of treated high-grade gliomas: tumor recurrence versus radiation injury.** *AJNR Am J Neuroradiol* 2004;25:201–09
45. Lidar Z, Mardor Y, Jonas T, et al. **Convection-enhanced delivery of paclitaxel for the treatment of recurrent malignant glioma: a phase I/II clinical study.** *J Neurosurg* 2004;100:472–79
46. Hamstra DA, Chenevert TL, Moffat BA, et al. **Evaluation of the functional diffusion map as an early biomarker of time-to-progression and overall survival in high-grade glioma.** *Proc Natl Acad Sci U S A* 2005;102:16759–64
47. Moffat BA, Chenevert TL, Lawrence TS, et al. **Functional diffusion map: a noninvasive MRI biomarker for early stratification of clinical brain tumor response.** *Proc Natl Acad Sci U S A* 2005;102:5524–29